EVALUATION OF NON-LINEAR ELASTIC AND PIEZOELECTRIC PROPERTIES OF $La_3Ta_{0.5}Ga_{5.5}O_{14}$ SINGLE CRYSTALS UNDER HYDROSTATIC PRESSURE

C. Hubert[1,*], M. Gauthier[1], F. Decremps[1], G. Syfosse[1], P. Munsch[2], A. Polian[1], E. Bigler[3] and J. J. Boy[3]
[1]Physique des Milieux Condensés, CNRS UMR 7602, Université Pierre et Marie Curie, Paris, France
[2]L.U.R.E., CNRS UMR 130, Centre Universitaire Paris-Sud, Orsay, France
[3]L.C.E.P., E.N.S.M.M., Besancon, France
[*]Email: christophe.hubert@pmc.jussieu.fr

Abstract

Two different elastic properties measurements of piezoelectric single crystals of $La_3Ta_{0.5}Ga_{5.5}O_{14}$ (LTG) are presented and compared in this paper.
The equation of state (EOS) of LTG was studied under hydrostatic pressure up to 20 GPa in diamond-anvil cell by powder X-rays diffraction. No structural transition was observed. The complete set of second order elastic constants (S.O.E.C) of LTG and their pressure derivatives were measured under hydrostatic pressure in Paris-Edinburgh press up to 8 GPa using ultrasonic measurement technique. Piezoelectric constants and the pressure derivative of e_{11} were deduced from this measurements. Bulk moduli and their initial pressure derivatives are calculated and compared with values obtained by fitting a Murnaghan EOS to the X-rays diffraction data. The Born criteria for crystal stability have been computed and compared with those of quartz.

Introduction

$La_3Ta_{0.5}Ga_{5.5}O_{14}$ (LTG) belongs to the Langasite (LGS) family (Trigonal symmetry, group point 32)[1] a large set of new piezoelectric crystals. Among them LTG is one of the most promising members since it exhibits the best technical characteristics for the development of efficient surface and bulk acoustic wave devices (SAW, BAW): moderate-high piezoelectric coupling coefficient, low acoustic loss, temperature compensation. Moreover, LTG possesses a high melting temperature (1500 $^\circ$C) and could be used to develop devices working under extreme conditions. The aim of our study is to investigate the LTG structural stability under pressure. Two high pressure studies on LTG were performed and are presented.

Equation of state

Crystal structure

LTG crystallizes in the trigonal $Ca_3Ga_2Ge_4O_{14}$ structure type with space group P321 [1]. From a general point of view, the structure type appears to be very close to quartz, but their space groups are different ($P3_121$ for quartz) and no helicoidal structure (observed in quartz) exists in LTG. The crystal structure can be described as a mixed framework consisting of layers of tetrahedra sharing corners, which are aligned perpendicular to the crystallographic c axis, sandwiched between octahedral-decahedral layers [2][3]. At ambient pressure, the cell parameters of LTG are a_0=8.228 Å and c_0=5.124 Å.

Experimental setup and results

The determination of the equation of state of LTG was performed by energy dispersive X-rays diffraction technique at LURE synchrotron on powder sample. Two different setups were used. In low-pressure range (0-7 GPa) the Paris-Edinburgh Press have been used with a special gasket including a furnace[4] in order to relax uniaxial stress under pressure by in situ high-temperature control of a mix powder of LTG and NaCl. Temperature was evaluated thanks to furnace calibration and pressure was measured by X-Rays diffraction on NaCl, whose EOS is a pressure standard [5]. For higher pressure range (0-20 GPa) a classical membrane diamond anvil cell (DAC) loaded with argon as pressure transmitting medium have been used. Quasi-hydrostatic stresses on the sample can be assumed in the whole pressure range. Pressure was measured with the ruby luminescence scale [6]. The pressure dependencies of the relative lattice parameters (a/a_0 and c/c_0) are plotted on Fig. 1. The results obtained by Werner

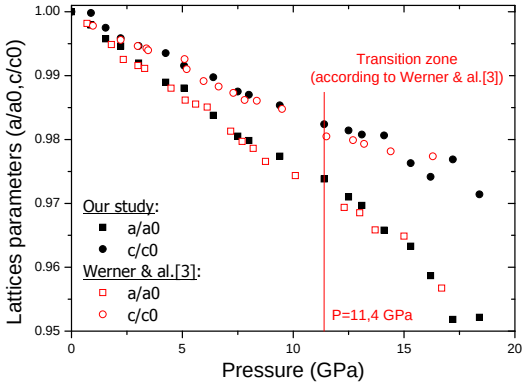

Figure 1: Relative variation of lattice parameters of LTG

et al.[3] are also plotted for comparison. In the pressure range from atmospheric to 12 GPa, the bulk modulus B_0 and the linear moduli B_a, B_c and their pressure derivatives at "zero pressure" have been obtained by fitting the Murnaghan equation of state to the data (Table 1). Results obtained with the Paris-Edinburgh press experiment setup are in good agreement with those obtained by the DAC one. There is an important anisotropic compression for the the c and a axis: the crystal lattice is less stiff perpendicular to the A3 axis. This difference of compressibility between the lattice parameters may be explained by the fact that octahedra sites are less compressible than tetrahedra ones. Lattice parameters have been refined in trigonal system on the whole pressure range. At variance with Werner et al.[3] who proposed a phase transformation from trigonal to monoclinic system at 11.4 GPa no transition has been observed.

Table 1: X-ray determination of Bulk Moduli of LGT

Modulus	(GPa)	derivative
B_0 (This work)	140(10)	3.0(2)
B_0 (Werner et al.[3])	144(2)	0.5(5)
B_a	370(8)	6.7(6)
B_c	604(8)	9.5(6)

Ultrasonic measurements

Principle

A piezoelectric crystal which belongs to the trigonal (32) system possess six independent elastic constants and also two piezoelectric constants (e_{11}, e_{14}). According to elasticity theory, the Christoffel equation has been solved for several wave propagation directions in the crystal. Corresponding elastic moduli expressions are resumed in the table 2. At least six different measurement directions are needed to obtain the complete set of S.O.E.C. and two others for piezoelectric constants. Nevertheless, for a better determination of C_{ij} and e_{ij}, all directions presented in the table 2 were investigated and results were fitted with an "inverse Monte Carlo" method to obtain a unique set of constants. S.O.E.C. combinations are obtained as the following relation :

$$C_{ij} = \rho V^2 = 4\rho \frac{L^2}{t^2} \qquad (1)$$

where ρ(kg/m^3) is the density , L(m) the sample length and t(s) the round travel time.

Experimentally, ultrasonic measurements consist in measuring the round travel time of a wave in a direction of the single crystal sample by a pulse-echo superposition method [7] with a pulser/receiver system coupled with an oscilloscope. Accuracy (1ns) was improved by the employment of a signal cross-correlation technique. Under pressure, density and length evolution are required to calculate elastic constants. Methods developed by Thurston or Cook [8] to calculate elastic constant from the time of flight experiments without equation of state are very tricky even for for cubic system and are irrelevant for low symmetry ones. A new "self-consistent" method has been developed to calculate elastic constant under pressure with only pressure derivatives of transit time. This method has been validated with quartz data according to McSkimin experiments[9].

Experimental setup

Single crystal samples were oriented and cut with various dimensions ranging from 4.97 to 6.93 millimeters (see ref [7] for the orientation definitions). Their density value at ambient pressure is ρ=6126 kg/m^3.
At ambient pressure, constants have been determined with a transducer mounted directly on the crystal along all directions. Measurements have been performed with many different sample and a unique elastic constants set has been determined. Results for S.O.E.C. and moduli at ambient pressure are summarized in Tab 3 & 4.
For high-pressure measurement, two different setups have been used. The "Low pressure acoustic measurement setup" used up to 1 GPa is shown on Fig. 2. Pressure was measured thanks to the variation of the resistivity of a manganin gauge. The sample holder maintains the LiNbO3 transducer mounted on the crystal providing direct echoes measurement from the sample. All is completely immersed in penthane, used as pres-

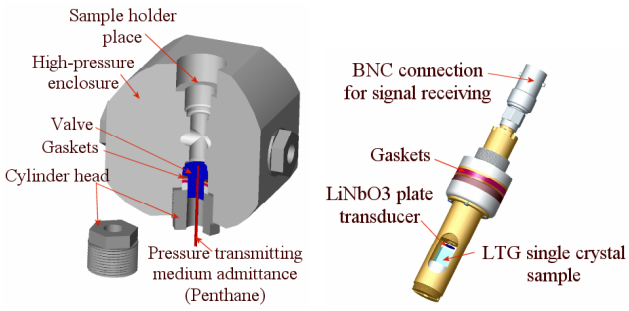

Figure 2: Low-pressure acoustic measurement setup (0-1 GPa) (Vessel and sample holder)

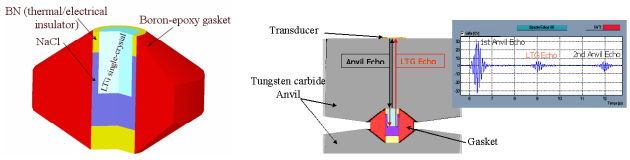

Figure 3: High-pressure acoustic measurement gasket (1-8 GPa) and wave path in the setup

Table 2: The effective second-order elastic constants (C_{ij}) of LTG. $Y'/+45^\circ$ and $Z'/-45^\circ$ correspond to propagation directions in the (100) plane at 45 ° and -45 ° to the Y axis respectively. e_{ij} and ϵ_{ij} designate piezoelectric and dielectric tensors. L and S stands for longitudinal and shear waves, QL, QS for the corresponding quasi-waves.

Exp.	q[$q_x q_y q_z$]	u[$u_x u_y u_z$]	Mode	ρV^2
1	X [100]	X	L	$C_{11}+\frac{e_{11}^2}{\epsilon_{11}}$
2	X [100]	(100) 32 °/Z	FS	$\frac{C_{66}+C_{44}}{2}+\frac{1}{2}\sqrt{(C_{66}-C_{44})^2+4C_{14}^2}$
3	X [100]	(100) 32 °/Y	SS	$\frac{C_{66}+C_{44}}{2}-\frac{1}{2}\sqrt{(C_{66}-C_{44})^2+4C_{14}^2}$
4	Y [010]	X	S	$C_{66}+\frac{e_{11}^2}{\epsilon_{11}}$
5	Y [010]	(100) 5 °/Y	QL	$\frac{C_{44}+C_{11}}{2}+\frac{1}{2}\sqrt{(C_{44}-C_{11})^2+4C_{14}^2}$
6	Y [010]	(100) 5 °/Z	QS	$\frac{C_{44}+C_{11}}{2}-\frac{1}{2}\sqrt{(C_{44}-C_{11})^2+4C_{14}^2}$
7	Z [001]	Z	L	C_{33}
8	Z [001]	(001)	S	C_{44}
9	$Y'/+45^\circ$	X	S	$\frac{C_{66}+C_{44}}{2}+C_{14}+\frac{(e_{11}+e_{14})^2}{2(\epsilon_{11}+\epsilon_{33})}$
10	$Y'/+45^\circ$	(100) 10 °/Y′	QL	$\frac{C_{11}+C_{33}+2C_{44}-2C_{14}}{4}+\frac{1}{2}\sqrt{\frac{(C_{11}-C_{33}-2C_{14})^2}{4}+(C_{44}+C_{13}-C_{14})^2}$
11	$Y'/+45^\circ$	(100) 10 °/Z′	QS	$\frac{C_{11}+C_{33}+2C_{44}-2C_{14}}{4}-\frac{1}{2}\sqrt{\frac{(C_{11}-C_{33}-2C_{14})^2}{4}+(C_{44}+C_{13}-C_{14})^2}$
12	$Y'/-45^\circ$	X	S	$\frac{C_{66}+C_{44}}{2}-C_{14}+\frac{(e_{11}-e_{14})^2}{2(\epsilon_{11}+\epsilon_{33})}$
13	$Y'/-45^\circ$	(100) 4 °/Z′	QL	$\frac{C_{11}+C_{33}+2C_{44}+2C_{14}}{4}+\frac{1}{2}\sqrt{\frac{(C_{11}-C_{33}+2C_{14})^2}{4}+(C_{44}+C_{13}+C_{14})^2}$
14	$Y'/-45^\circ$	(100) 4 °/Y′	QS	$\frac{C_{11}+C_{33}+2C_{44}+2C_{14}}{4}-\frac{1}{2}\sqrt{\frac{(C_{11}-C_{33}+2C_{14})^2}{4}+(C_{44}+C_{13}+C_{14})^2}$

Table 3: Elastic piezoelectric and dielectric constants at ambient pressure (C_{ij} in GPa, e_{ij} in C/m^2)

Ref.	C_{11}	C_{12}	C_{13}	C_{14}	C_{33}	C_{44}	C_{66}	B_0	B_a	B_c	e_{11}	e_{14}	ϵ_{11}/ϵ_0	ϵ_{33}/ϵ_0
This work	191.4(3)	115.4(5)	103.3(3)	13.1(1)	267.1(1)	51.0(1)	38.0(1.5)	141.7	370	604	-0.6(0.1)	-0.07(?)	19.6	76.5
Ref.[10]	188.9	108.1	100.8	13.9	264.4	51.2	40.4	137.7	355.8	610.1	-0.508	-0.028	19.6	76.5
Ref.[1]	190.9	107.9	73.9	13.7	263.2	51.2	41.5	127.9	357.7	448.5	-0.54	0.07(?)	18.5	60.9
Ref.[11]	202	120	125	13.3	288	49.7	40.7	154.5	377.2	854	-0.468	0.0632	19.3	80.3
LGS [1]	189.3	105	95.3	14.93	262.4	53.84	42.16	134.9	353.4	569.5	-0.431	-0.108	18.97	52

Table 4: Pressure derivatives of elastic and piezoelectric constants

$\frac{\partial C_{11}}{\partial P}$	$\frac{\partial C_{12}}{\partial P}$	$\frac{\partial C_{13}}{\partial P}$	$\frac{\partial C_{14}}{\partial P}$	$\frac{\partial C_{33}}{\partial P}$	$\frac{\partial C_{44}}{\partial P}$	$\frac{\partial C_{66}}{\partial P}$	$\frac{\partial B_0}{\partial P}$	$\frac{\partial B_a}{\partial P}$	$\frac{\partial B_c}{\partial P}$	$\frac{\partial e_{11}}{\partial P}$
+6.92(0.1)	+4.39(0.5)	+4.55(0.1)	-0.05(0.01)	+5.63(0.1)	+0.57(0.1)	+1.27	+5.25(0.1)	+15.11(0.5)	+15.11(0.5)	-0.05(0.03)

sure transmitting medium so that the sample undergoes a perfectly hydrostatic strain. The second setup designed for high pressure (up to 8 GPa) investigations is described on Fig. 3. The gasket is compressed with the Paris-Edimbourg press and pressure is measured by X-rays diffraction on NaCl [5]. A transducer was mounted on backside of the superior anvil, the travel time in the sample being measured by superposition of the anvil and the sample echoes (Fig. 3).

Experimental results and discussion

The results obtained at ambient pressure (Table 3) are in good agreement with previous publications except for C_{13} for which only values obtained by [10] is close to our. Bulk modulus and linear moduli computed from C_{ij} are in good agreement with X-rays experiment results.

Under pressure, the travel time measured in the sample shows a linear regression with pressure. The natural velocities plotted in fig. 4 & 5 are expressed as following:

$$W_0 = 2\frac{L(P=0)}{t(P=0)} \quad W = 2\frac{L(P=0)}{t(P)} \qquad (2)$$

Pressure derivatives of S.O.E.C. and of piezoelectric constant e_{11} have been computed with the new not yet publish "self-consistent" method (Table 4). The pressure derivative of the bulk and linear moduli have been calculated with our results. All the pressure derivatives of S.O.E.C. are positives except for the C_{14}. The first derivatives versus pressure for bulk and linear moduli

disagree with those obtained by X-rays diffraction. The mechanical stability of LTG crystal under pressure can be evaluated with the Born criteria stability B_1, B_2, B_3 [12]. In case of LTG, all pressure derivatives of these criteria have been found positives. Thus, no ferroelastic phase transition is expected.

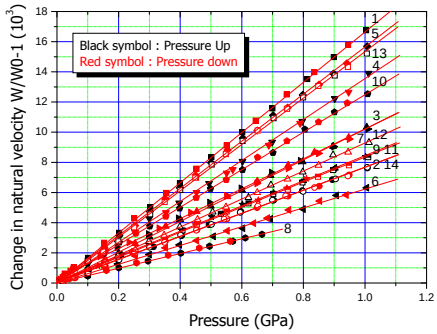

Figure 4: Relative Change in the natural wave velocity induced by application of hydrostatic pressure. (Labels as in the table 2).

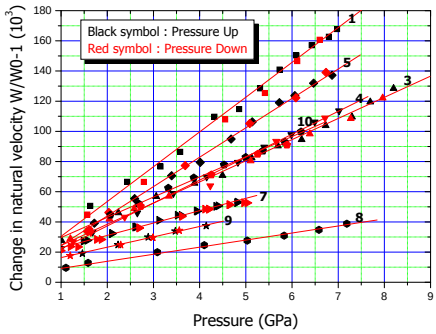

Figure 5: Relative Change in the natural wave velocity induced by application of pseudo-hydrostatic pressure (Labels as in the table 2).

Conclusions

The equation of state of LTG has been determined with X-rays diffraction technique up to 20 GPa. No phase transition has been observed. Thanks to several ultrasonic measurements performed on LTG under pressure, the complete elastic behavior is known. According to Born-criteria stability, no precursor of the transition reported by Werner et al. have been observed.

References

[1] B.V. Mill & Y.V. Pisarevsky, ”Langasite-type materials: From discovery to present state”, Proceedings of IEEE/EIA International Frequency Control Symposium, pp. 133-148, 2000.

[2] H. Takeda et al., ”Crystal growth and structural Characterization of new piezoelectric material $La_3Ta_{0.5}Ga_{5.5}O_{14}$”, Japanese Journal of Applied Physics, Vol. 36, Part. 2, pp. 919-921, 1997.

[3] S. Werner et al., ”Pressure-induced phase transition of piezoelectric single crystals from the langasite family: $La_3Nb_{0.5}Ga_{5.5}O_{14}$ and $La_3Ta_{0.5}Ga_{5.5}O_{14}$”, Acta Crystallographica S. B, Vol. B58, pp 939-947, 2002.

[4] Y. Le Godec, ”Etude du nitrure de bore sous hautes pression et temperature”, PhD Thesis, University Denis Diderot, Paris, 1999.

[5] D.L. Decker, ”High-pressure equation of state for NaCl, KCl and CsCl”, Journal of Applied Physics, Vol. 42, pp. 3239-3244, 1971.

[6] G. J. Piermarini et al., ”Calibration of the pressure dependence of the R/sub 1/ ruby fluorescence line to 195 kbar”, Journal of Applied Physics, Vol. 46, pp. 2774-2780, 1975.

[7] H. A. A. Sidek et al., ”Elastic behavior under hydrostatic pressure and acoustic vibrationnal anharmonicity of single-crystal berlinite”, Physical Review B, Vol. 36, pp. 7612-7613, 1987.

[8] D. Lheureux, ”Proprietes elastiques non lineaires sous pression et diagramme de phase du titanate de strontium”, PhD Thesis, University Pierre et Marie Curie, Paris, 2000.

[9] H. J. McSkimin et al., ”Elastic moduli of quartz versus hydrostatic pressure at 25 $^\circ$C and -195.8 $^\circ$C”, Journal of Applied Physics, Vol. 36, pp. 1624-1632, 1965.

[10] E. Chilla et al., ”Elastic properties of langasite-type crystals determined by bulk and surface acoustic wave”, Journal of Applied Physics, Vol. 90, pp. 6084-6091, 2001.

[11] N. Onazoto et al., Japanese Journal of Applied Physics, Vol. 39, pp. 3028, 2000.

[12] N. Binggeli et al., ”Pressure-induced amorphization, elastic instability, and soft modes in α-quartz”, Physical Review B, Vol. 49, pp. 3075-3081, 1994.